Roughness evolution during the atomic layer deposition of metal oxides

Peter Antony Premkumar, Annelies Delabie, Leonard N. J. Rodriguez, Alain Moussa, and Christoph Adelmann[a)]
Imec, B-3001 Leuven, Belgium

(Received 12 March 2013; accepted 18 June 2013; published 2 July 2013)

The evolution of the surface roughness during the atomic-layer deposition (ALD) of Al_2O_3, NiO, and HfO_2 was studied by atomic-force microscopy and nonspecular x-ray reflectance. The results indicate that the crystallinity of the films played a crucial role in the roughness evolution during ALD. While the ALD of amorphous oxide films showed replication of the initial starting surface with no roughness build-up, the ALD of polycrystalline oxide films led to a strong anomalous dependence of the roughness on the film thickness. This behavior is explained within a model taking into account spatial variations of the adsorption site density. © *2013 American Vacuum Society*.
[http://dx.doi.org/10.1116/1.4812707]

I. INTRODUCTION

In recent years, atomic-layer deposition (ALD)[1,2] has become the reference technique for the deposition of dielectric[3] and metallic[4] thin films for nanoelectronic,[5–7] photovoltaic,[8] or energy storage applications.[9–11] The main advantage of ALD lies in its ability to deposit high-quality thin films with outstanding process control at low temperatures. In addition, the excellent conformality of the resulting thin films allows for their deposition onto three-dimensional structures, as required for numerous advanced device applications.

The main underlying principle of ALD is the usage of self-saturating adsorption and reaction of the precursors. A generic ALD process consists of the self-saturating adsorption of a precursor from the vapor phase onto the substrate surface followed by a purge of the excess precursor vapor. This results in a monolayer or submonolayer of chemisorbed precursor on the surface. Subsequently, the chemisorbed (sub-)monolayer is reacted into the target material by the exposure to a second precursor vapor. This step is also self-limiting, and the excess of the second precursor can also be subsequently purged. The sequence can be repeated to deposit thicker films. In an ideal ALD process, the amount of material deposited in each cycle (growth per cycle, GPC) is constant and independent of variations of the precursor doses due to the self-limiting nature of the chemisorption and reaction processes. This leads to the excellent process control and to the conformality of the deposited films.

Although a key enabling technique for many nanotechnology applications, the fundamental growth physics of ALD—and in particular the evolution of the surface roughness—has received less systematic attention so far.[12–14] The surface chemistry of selected processes, in particular, the ALD of Al_2O_3 using trimethylaluminum [TMA, $Al(CH_3)_3$] and H_2O, has been studied in detail.[1,2,15] Detailed work has also been devoted to the initial nucleation in heterodeposition and the repercussions on the initial GPC.[16]

Beyond the initial nucleation, the further evolution of the surface morphology is a key parameter to describe any deposition process. In the past, the evolution of the morphology has been studied both theoretically[17–19] and experimentally for numerous deposition methods.[20,21] Calculations have also been performed for ALD[22] using a cyclic random deposition model. However, a detailed experimental study of the morphology evolution during ALD is lacking. In this article, we discuss the evolution of the surface morphology during the ALD of three different metal oxides, Al_2O_3, NiO, and HfO_2. We show that the roughness evolution during ALD depended critically on the crystallinity of the films. For *amorphous* oxides, the roughness was fully independent of the film thickness. By contrast, the ALD of *polycrystalline* oxides showed an anomalous behavior with the root-mean-square (rms) surface roughness $\sigma(t)$ increasing according to $\sigma(t) \propto t^\beta$ with process-dependent $\beta > 0.5$. Thus, ALD does not fit into any common universality class.[17,18,23]

II. EXPERIMENTAL DETAILS

All samples have been grown on 300 mm Si(100) wafers. Prior to ALD, a 1.0 nm thick SiO_2 layer was grown on the wafers by rapid thermal oxidation. Al_2O_3 and HfO_2 were deposited in an ASM Pulsar 3000® reactor from TMA and $HfCl_4$, respectively,[2] in combination with H_2O. The deposition temperature was 300 °C for both processes. NiO was deposited in a TEL Trias® reactor from dimethylamino-methyl-butanolate nickel [$Ni(dmamb)_2$] and O_3 at 200 °C.[24] The film thickness and crystallinity were determined by x-ray reflectivity (XRR) and grazing-incidence x-ray diffraction (GIXRD, $\omega = 1°$), respectively, using a Jordan Valley MetrixL diffractometer. Nonspecular x-ray reflectivity (NS-XRR) was performed in a PANalytical X'Pert Pro diffractometer. In all cases, Cu Kα radiation was used. Modeling of the NS-XRR was done within the distorted-wave Born approximation (DBWA)[25] using the PANalytical X'Pert Reflectivity software. Both the rms roughness and the lateral correlation lengths were obtained from simultaneous modeling of NS-XRR for $2\Theta = 1°$ and $2\Theta = 2°$, as well as XRR. Atomic force microscopy (AFM) was carried out in a Nanoscope IVa from Veeco Instruments. The AFM micrographs were analyzed using the Gwyddion software.[26] The lateral correlation length was extracted through the autocorrelation function.

[a)]Electronic mail: christoph.adelmann@imec.be

Author complimentary copy. Redistribution subject to AIP license or copyright, see http://jva.aip.org/jva/copyright.jsp

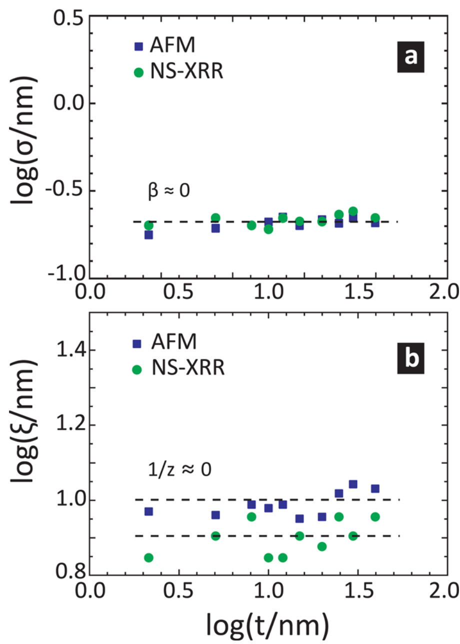

FIG. 1. (Color online) (a) Logarithms of the rms roughness σ and (b) the correlation length ξ for of atomic-layer deposited Al_2O_3 as a function of the logarithm of the film thickness.

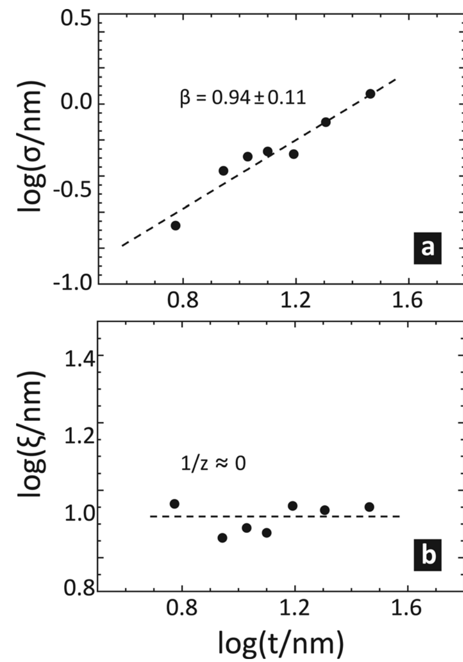

FIG. 2. (a) Logarithms of the rms roughness σ and (b) the correlation length *xi* for NiO as a function of the logarithm of the film thickness.

III. RESULTS AND DISCUSSION

Figure 1 shows the evolution of the rms surface roughness, σ, during the ALD of Al_2O_3 for film thicknesses up to 39.8 nm. GIXRD indicated that all films were amorphous. Both NS-XRR and AFM[27] showed consistently that $\sigma \sim 0.3$ nm, with no apparent increase with the film thickness. The Al_2O_3 ALD process is thus characterized by a scaling exponent of $\beta \approx 0$. Both AFM and NS-XRR also showed consistently that the lateral correlation length was of the order of $\xi \sim 8-10$ nm, again independent of the film thickness, and thus $\xi(t) \propto t^{1/z}$ with an exponent of $1/z \simeq 0$.

Both the rms value ($\sim$0.3 nm) as well as the lateral correlation length of the Al_2O_3 films were close to the values observed for the 1 nm SiO_2 starting surface ($\sigma = 0.23$ nm, $\xi \sim 10$ nm).[27] As a result, the ALD of amorphous Al_2O_3 can be classified as "ultraconformal," in the sense that it preserves the characteristic length scales of the starting surface even on a nanoscale. This will be discussed in more detail later.

By contrast, all NiO films with thicknesses from 6.0 to 29.3 nm were polycrystalline, as per GIXRD. No signs of texture were detected in any of the films. The evolution of the rms roughness σ of NiO films showed a distinct thickness dependence, as demonstrated in Fig. 2(a) from AFM measurements.[27] A rapid increase of σ with the film thickness was observed, characterized by an anomalous scaling exponent of $\beta = 0.94 \pm 0.11$. By contrast, Fig. 2(b) shows that the lateral correlation length did not depend on the film thickness; hence $1/z \simeq 0$ also for NiO.

For HfO_2, the evolution of the rms roughness σ [Fig. 3(a)] and the lateral correlation length ξ [Fig. 3(b)] were influenced by an amorphous-to-polycrystalline transition around 12 nm.[27,28] While thin films were x-ray amorphous, films thicker than $\sim$12 nm showed a mixture of the monoclinic and cubic phases of HfO_2. This transition is replicated in the evolution of σ and ξ.[27] The data showed only a weak increase of $\sigma \sim 0.3$ nm and $\xi \sim 8$ nm in the amorphous range up to $\sim$12 nm. For thicker films, both σ and ξ increased as the growth proceeded as polycrystalline films. Best fits to data for thicknesses >10 nm using $\sigma \propto (t - t_0)^{\beta'}$ and $\xi \propto$

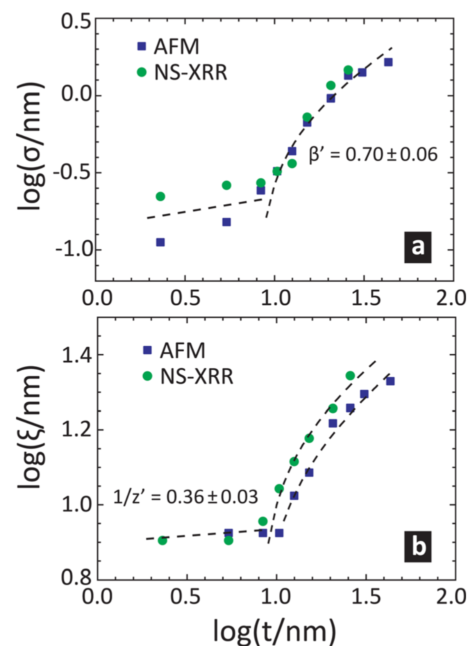

FIG. 3. (Color online) (a) Logarithms of the rms roughness σ and (b) the correlation length ξ for HfO_2 as a function of the logarithm of the film thickness.

Author complimentary copy. Redistribution subject to AIP license or copyright, see http://jva.aip.org/jva/copyright.jsp

$(t - t_0)^{1/z'}$ led to $\beta' = 0.70 \pm 0.06$ and $t_0 = 8$ nm. There was a moderate correlation between β' and t_0, but for all realistic values of t_0, β' was anomalous (>0.5), as for NiO. The difference between t_0 and the transition thickness in GIXRD (~12–15 nm) may be due to the limited sensitivity of GIXRD to small and/or sparse crystallites. Similarly, we found $1/z = 0.36 \pm 0.03$ from both NS-XRR and AFM (with $t_0 = 8$ nm and only slightly varying prefactors). Hence the results consistently show that the ALD of amorphous oxide films and polycrystalline films fall in clearly distinct classes. While the former is characterized by a small value of $\beta \simeq 0$, the latter leads to $\beta > 0.5$.

The paramount significance of the crystallinity for the roughness evolution was also corroborated by the behavior of Al_2O_3–HfO_2 multilayers. These multilayers were found to be x-ray amorphous. The x-ray reflectance pattern of an eightfold Al_2O_3–HfO_2 multilayer is shown in Fig. 4(a). Excellent agreement with the experimental data could be achieved by a multilayer model with individual layer thicknesses of 4.6 nm for Al_2O_3 (interface roughness $\sigma = 0.31$ nm) and 4.4 nm for HfO_2 ($\sigma = 0.34$ nm). In this multilayer model, all layers could be described by identical parameters. These results indicate that the roughness did not increase during the deposition of the multilayer although the total film thickness of the multilayer exceeded 70 nm.[29] In particular, this indicates that the absolute total HfO_2 thickness (~35 nm in the multilayer) became irrelevant for the roughness evolution when the individual HfO_2 layers (4.4 nm) remained amorphous because of the increased crystallization barrier for such thin films.[30]

In addition, the NS-XRR reciprocal space map in Fig. 4(b) indicated that the roughness in the multilayer was also spatially correlated. The appearance of curved peaks ["RDS bananas," see arrow in Fig. 4(b)], which stem from resonant enhancement of the diffuse reflectance, demonstrates that the interface roughness was replicated.[31] Simulations of the intensity of the RDS bananas within the DBWA as well as their narrow width suggest that the degree of correlation was very high. This further underlines the ultraconformal nature of the ALD of amorphous oxides, which replicates the starting surface on a nanoscale.[32]

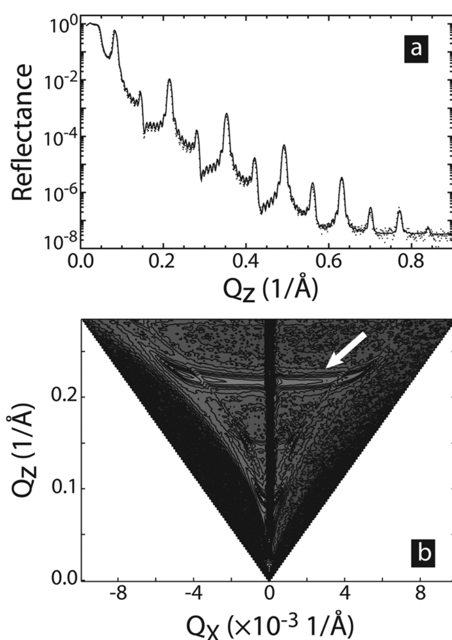

Fig. 4. (a) Specular and (b) nonspecular x-ray reflectance of an 8-period HfO_2/Al_2O_3 multilayer. In (a), the solid line is a best fit to the data using the structure described in the text.

For conventional deposition methods, the surface roughening and the morphology evolution during growth stems from statistical noise on the impinging flux in combination with smoothening effects, e.g., due to diffusion. Ultrasmooth growth with $\beta = 0$ has been linked to anisotropic downhill particle flows, e.g., as described by the two-dimensional Edwards–Wilkinson model.[17,18] By contrast, the structure of the layer deposited by one ALD cycle depends only on the structure of the saturated adsorbate layer of the precursors. The adsorbate density in saturation may be influenced by diffusional relaxation in the random sequential adsorption process.[33] Nonetheless, if the adsorption sites are spatially uniform, the adsorbate (and thus the layer) will be uniform on all length scales beyond a few adsorption site distances or length scales of jamming fluctuations in the case of steric hindrance.

As a result, the equivalent "flux" in ALD does not show any spatial fluctuations beyond subnanometer scales, which are not probed in our experiments. Random deposition is thus not applicable to ALD, in contrast to previous attempts to model the ALD growth.[22] Since also temporal fluctuations are zero for cyclic saturated adsorption, the ALD flux is "noiseless" and does not lead to kinetic roughening. It is also clear that ALD will replicate the substrate roughness on all length scales beyond molecular length scales. This explains the absence of coarsening during the ALD of Al_2O_3 as well as the correlation of the interface roughness in the Al_2O_3–HfO_2 multilayer.

Although the above discussion describes in principle a generic ALD process, the experimental results indicate that the noiseless-flux argument appears only valid for the ALD of amorphous oxide films. By contrast, the ALD of polycrystalline oxides was characterized by anomalous exponents $\beta > 0.5$, *i.e.* by ultrafast roughening. Previously, values of $\beta > 0.5$ have often been attributed to shadowing effects;[34] however, because of the conformal nature of ALD, such effects can be safely excluded. We believe that the ultrafast roughening during the ALD of polycrystalline oxides can be explained by spatial nonuniformity of the density of the adsorbed precursors. It is very plausible that the local density of adsorption sites on a polycrystalline film depends on the local surface orientation of the crystalline grains. Even when the GPC is strongly influenced by steric hindrance [e.g., as expected for the bulky $Ni(dmamb)_2$ molecules], it is plausible that this still the case, at least to some extent. For conventional deposition methods with a uniform flux, as long as the sticking probability is spatially uniform, the deposition rate will be uniform, as long the density of the deposited material is spatially uniform. By contrast, in ALD, the precursor doses are typically chosen to saturate any local density of

Author complimentary copy. Redistribution subject to AIP license or copyright, see http://jva.aip.org/jva/copyright.jsp

adsorbate sites. Hence, the ALD growth mode can allow for spatial variations of the deposition rate (the GPC) of films with uniform density.

The effect of a spatially nonuniform adsorbate density is to some extent equivalent to the effect of a grain-orientation-dependent sticking coefficient in conventional deposition methods. This has been discussed before in the literature as one of several mechanisms leading to textured growth of polycrystalline films.[35–37] In this case, the grains with the fastest growth rate(s) will eventually prevail, leading to films with a preferred out-of-plane orientation. Both the HfO_2 and NiO films considered in this work however did not show any preferred orientation for all thicknesses considered, as measured by x-ray diffraction. Note that this is also true for the HfO_2 films after the amorphous-to-crystalline transition at a film thickness of about 12 nm. It is however likely that the local growth rate variation in ALD will eventually lead to the formation of a preferred orientation for much thicker films. In our cases, the differences in the local adsorbate density (the local GPC) can be estimated from the surface width and the film thickness to be of the order of 10%. The formation of a preferred orientation will only occur when the local differences in total growth become comparable to the grain size. Even for the thickest of our samples, the roughness amplitude ($\approx$2 nm) is still much smaller than the typical grain size ($\approx 6-8$ nm for NiO and $\approx 20-30$ nm for thick HfO_2).

It is straightforward to calculate the roughness evolution of a surface with local growth rate variations analytically; in all cases, $\sigma \propto t$, i.e., $\beta = 1$. We believe that this growth regime was realized during the ALD of NiO, where a value of $\beta = 0.94$ was observed. If one assumes that there the crystallite size did not significantly change during deposition ("columnar growth"), $1/z \simeq 0$, as also experimentally observed for NiO. This is consistent with the observation that the Scherrer grain size extracted from GIXRD pattern (6–8 nm) was rather independent of the film thickness.[24] This suggests that the roughening of NiO cannot be ascribed to the coarsening of grains in the bulk. We also note that such a growth mode (i.e., without "lateral" grain growth) is not inconsistent with the conformality of ALD as long as the maximum surface corrugation remains much smaller than the grain size, which was indeed the case for NiO in the studied thickness range.

By contrast, the crystalline structure (and crystallite size) of HfO_2 changes strongly as a function of the film thickness, as indicated by the amorphous-to-polycrystalline transition around film thicknesses of 12 nm. In such a case, one would expect $1/z > 0$, as observed for HfO_2. A comprehensive model of ALD on a surface with an evolving nonuniformity of surface sites is beyond the scope of the paper. Because the deposition temperature is comparable to the crystallization temperature for HfO_2 films in the studied thickness range, both bulk diffusion and grain growth may have to be considered, surpassing pure surface growth models. Such a deposition process may also not be described by a polynominal behavior with a single exponent. However, for large thicknesses, the fastest growing grains will dominate, and the relative variation of the growth rate on the surface should decrease. This is expected to slow down the roughening with respect to $\beta = 1$ for a constant microstructure, qualitatively consistent with the experimental data for HfO_2, for which $\beta = 0.70$ was obtained.

IV. CONCLUSION

In conclusion, it has been shown that ALD can lead to both ultrasmooth and ultraconformal growth with a roughening exponent of $\beta = 0$, provided that the density of adsorption sites is spatially uniform. This is realized in the ALD of amorphous Al_2O_3 and approximately for thin ($\ll$10 nm) amorphous HfO_2, as demonstrated above.[38] As a result, the initial surface roughness is replicated by the ALD layer, even on a nanoscale, leading to strong correlations between interface morphologies in multilayers. Here, neither the magnitude nor the correlation length of the surface roughness is related to any intrinsic parameter of the ALD process but only to the surface properties of the substrate. We emphasize that the behavior of the ALD of amorphous metal oxide films is not intrinsically linked to the amorphous microstructure[38]—only the spatial uniformity of the adsorption sites.

By contrast, the ultrafast roughening with exponents of $\beta > 0.5$ for polycrystalline oxides indicates that the assumption of a spatially uniform adsorption—and thus a spatially uniform GPC—is not necessarily always fulfilled. This leads to a different mechanism for surface roughening characterized—in the absence of lateral grain growth—by $\beta = 1$. Additional lateral grain growth appears to reduce the roughening rate. The data indicate that the typical local variations of the GPC are of the order of 10% for both NiO and HfO_2, and thus much lower than "geometric" factors based on typical atomic densities of low-index crystallographic facets. If lateral grain growth is present, the GPC may also become non-constant during ALD; however, for HfO_2, this effect will be only of the order of a few percent at most, difficult to unambiguously observe in experiments. It will however be interesting to examine other ALD processes of polycrystalline oxides for larger differences in local GPC.

Previously, roughening in ALD was often linked to island nucleation and growth;[12,13] however, this is not a necessary condition since two-dimensional nucleation and rapid film closure was also observed for the ALD of polycrystalline films. We also note that the roughening does not stem from the kinetics of the growth only since all surface structures are in equilibrium. These results demonstrate that the growth modes of ALD can be rather diverse and that surface roughening dynamics are a powerful tool to elucidate mechanisms of ALD deposition, which are not readily accessible by other direct measurements due to the small length scales involved.

ACKNOWLEDGMENTS

The authors would like to thank Michael Toeller for experimental help with the NiO ALD. Leonard Rodriguez' work was partially funded by a Marie Curie International Reintegration Grant (IRG) under Call No. FP7-PEOPLE-2010-RG.

Author complimentary copy. Redistribution subject to AIP license or copyright, see http://jva.aip.org/jva/copyright.jsp

[1]S. M. George, Chem. Rev. **110**, 111 (2010).
[2]R. L. Puurunen, J. Appl. Phys. **97**, 121301 (2005).
[3]M. Ritala, K. Kukli, A. Rahtu, P. I. Räisänen, M. Leskelä, T. Sajavaara, and J. Keinonen, Science **288**, 319 (2000).
[4]B. S. Lim, A. Rahtu, and R. G. Gordon, Nature Mater. **2**, 749 (2003).
[5]R. Chau, B. Doyle, S. Datta, J. Kavalieros, and K. Zhang, Nature Mater. **6**, 810 (2007).
[6]D.-H. Kwon *et al.*, Nature Nanotechnol. **5**, 148 (2010).
[7]A. Javey *et al.*, Nature Mater. **1**, 241 (2002).
[8]G. Agostinelli, A. Delabie, P. Vitanov, Z. Alexieva, H. F. W. Dekkers, S. De Wolf, and G. Beaucarne, Sol. Energy Mater. Sol. Cells **90**, 3438 (2006); B. Hoex, J. Schmidt, R. Bock, P. P. Altermatt, M. C. M. van de Sanden, and W. M. M. Kessels, Appl. Phys. Lett. **91**, 112107 (2007).
[9]P. Banerjee, I. Perez, L. Henn-Lecordier, S. B. Lee, and G. W. Rubloff, Nature Nanotechnol. **4**, 292 (2009).
[10]A. Paracchino, V. Laporte, K. Sivula, M. Grätzel, and E. Thimsen, Nature Mater. **10**, 456 (2011); Y. W. Chen, J. D. Prange, S. Dühnen, Y. Park, M. Gunji, C. E. D. Chidsey, and P. C. McIntyre, *ibid.* **10**, 539 (2011).
[11]Y. S. Jung, A. S. Cavanagh, L. A. Riley, S.-H. Kang, A. C. Dillon, M. D. Groner, S. M. George, and S.-H. Lee, Adv. Mater. **22**, 2172 (2010).
[12]J. W. Elam, Z. A. Sechrist, and S. M. George, Thin Solid Films **414**, 43 (2002).
[13]M. Ritala, M. Leskelä, L.-S. Johansson, and L. Niinistö, Thin Solid Films **228**, 32 (1993).
[14]S. M. George, A. W. Ott, and J. W. Klaus, J. Phys. Chem. **100**, 13121 (1996).
[15]M. M. Frank, Y. J. Chabal, and G. D. Wilk, Appl. Phys. Lett. **82**, 4758 (2003).
[16]M. L. Green *et al.*, J. Appl. Phys. **92**, 7168 (2002); R. L. Puurunen and W. Vandervorst, *ibid.* **96**, 7686 (2004); O. Nilsen, C. E. Mohn, A. Kjekshus, and H. Fjellvåg, *ibid.* **102**, 024906 (2007).
[17]A.-L. Barabási and H. E. Stanley, *Fractal Concepts in Surface Growth* (Cambridge University Press, New York, 1995).
[18]M. Pellicone and T.-M. Lu, *Evolution of Thin Film Morphology* (Springer, Berlin, Heidelberg, 2008).
[19]J. Krug, Adv. Phys. **46**, 139 (1997).
[20]H. You, R. P. Chiarello, H. K. Kim, and K. G. Vandervoort, Phys. Rev. Lett. **70**, 2900 (1993); H.-N. Yang, Y.-P. Zhao, G.-C. Wang, and T.-M. Lu, *ibid.* **76**, 3774 (1996); M. Pelliccione, T. Karabacak, C. Gaire, G.-C. Wang, and T.-M. Lu, Phys. Rev. B. **74**, 125420 (2006).
[21]F. Ojeda, R. Cuerno, R. Salvarezza, and L. Vázquez, Phys. Rev. Lett. **84**, 3125 (2000); A. Yanguas-Gil, J. Cotrino, A. Walkiewicz-Pietrzykowska, and A. R. González-Elipe, Phys. Rev. B **76**, 075314 (2007).
[22]R. L. Puurunen, Chem. Vap. Depos. **10**, 159 (2004); J.-H. Ahn, S.-H. Kwon, J.-H. Kim, J.-Y. Kim, and S.-W. Kang, J. Mater. Sci. Technol. **26**, 371 (2010).
[23]S. Das Sarma and S. V. Ghaisas, Phys. Rev. Lett. **69**, 3762 (1992).
[24]P. Antony Premkumar *et al.*, Chem. Vap. Depos. **18**, 61 (2012).
[25]S. K. Sinha, E. B. Sirota, S. Garoff, and H. B. Stanley, Phys. Rev. B **38**, 2297 (1988).
[26]D. Nečas and P. Klapetek, Centr. Eur. J. Phys. **10**, 181 (2012); Gwyddion version 2.13, available at www.gwyddion.net. Values for σ and ξ were obtained by analyzing and averaging over four micrographs of 2×2 μm^2 per sample.
[27]See supplementary material at http://dx.doi.org/10.1116/1.4812707 for AFM micrographs and NS-XRR pattern including best fits to the data.
[28]M. Ritala, M. Leskelä, L. Niinistö, T. Prohaska, G. Friedbacher, and M. Grasserbauer, Thin Solid Films **250**, 72 (1994).
[29]J. M. Jensen, A. B. Oelkers, R. Toivola, D. C. Johnson, J. W. Elam, and S. M. George, Chem. Mater. **14**, 2276 (2002).
[30]C. Adelmann, J. Kesters, K. Opsomer, C. Detavernier, J. A. Kittl, and S. Van Elshocht, Appl. Phys. Lett. **95**, 091911 (2009).
[31]V. Holý and T. Baumbach, Phys. Rev. B **49**, 10668 (1994); T. Baumbach and P. Mikulík, in *X-Ray and Neutron Reflectivity*, edited by J. Daillant and A. Gibaud (Springer, Berlin, 2010), Chap. 6, pp. 235.
[32]F. H. Fabreguette, R. A. Wind, and S. M. George, Appl. Phys. Lett. **88**, 013116 (2006).
[33]J. W. Evans, Rev. Mod. Phys. **65**, 1281 (1993).
[34]C. Roland and H. Guo, Phys. Rev. Lett. **66**, 2104 (1991).
[35]Y. Kajikawa, S. Noda, and H. Komiyama, Solid State Phenom. **93**, 411 (2003).
[36]Y. Kajikawa, J. Cryst. Growth **289**, 387 (2006).
[37]M. A. Auger, L. Vazquez, M. Jergel, O. Sanchez, and J. M. Albella, Surf. Coat. Technol. **180–181**, 140 (2004).
[38]C. Tang, S. Alexander, R. Bruinsma, and B. E. Shaw, Phys. Rev. Lett. **64**, 772 (1990).

Author complimentary copy. Redistribution subject to AIP license or copyright, see http://jva.aip.org/jva/copyright.jsp